



UNIUNEA EUROPEANĂ



GUVERNUL ROMÂNIEI  
MINISTERUL MUNCII, FAMILIEI,  
PROTECȚIEI SOCIALE ȘI  
PERSONELOR VÂRSTNICE  
AMPOSDRU



Fondul Social European  
POSDRU 2007-2013



Instrumente Structurale  
2007-2013



MINISTERUL  
EDUCAȚIEI  
NAȚIONALE  
OIPOSDRU



UNIVERSITATEA  
„ALEXANDRU IOAN CUZA”  
din IAȘI

“AL. I CUZA” UNIVERSITY OF IASSY  
FACULTY OF PHYSICS

*Contributions to the study of  
nanoparticles utilized as contrast agents  
in medical nuclear resonance imagery  
-Summary-*

**SCIENTIFIC COORDINATOR:**

Prof. Univ. Dr. Ovidiu Florin CĂLȚUN

**Ph.D STUDENT:**

Cristin-Petrică CONSTANTIN

**IASSY, September 2013**



For the attention of

---

“AL. I CUZA” UNIVERSITY OF IASSY

We inform you that on the 26<sup>th</sup> September 2013, at 10<sup>00</sup>h in the room L1, doctoral candidate Cristin-Petrică Constantin will present in open meeting her doctor degree dissertation entitled “Contributions to the study of nanoparticles utilized as contrast agents in medical nuclear resonance imagery” with the view to obtain the scientific PhD title of PhD.

The **Doctoral Commission** consists of:

**Chairman:**

*PhD Prof. Diana Mardare*, Faculty of Physics, „Al. I. Cuza”

University of Iassy

**Scientific Coordinator:**

*PhD Prof. Ovidiu-Florin Căltun*, Faculty of Physics, „Al.

I. Cuza” University of Iassy

**Referents:**

*PhD Prof. Alexandra-Raluca Iordan*, Faculty of Chemistry,  
“Al.I. Cuza” University of Iassy

*PhD Prof. Simion Simon*, Faculty of Physics, “Babes Bolyai”  
University of Cluj-Napoca

*PhD. Prof. Ioan Poiatǔ*, University of Medicine and Pharmacy  
“Gr. T. Popa” of Iassy

## Content

<b>Introduction</b>	6
<b>Chapter 1</b> Basic principles of NMR	7
1.1. Nuclear magnetic resonance	7
1.2. Larmour precession	8
1.3. Relaxation times. Bloch equations	8
1.3.1. Relaxation time T1	8
1.3.2. Relaxation time T2	8
1.4. Bloch equations	8
1.5. Fourier Transform	9
1.6. Imagine generation in magnetic resonance imagery	9
1.7. Space k	9
1.8. Artifacts in magnetic resonance imagery	9
1.9. NMR equipment used in medical diagnosis	10
<b>Chapter 2</b> State of art of researches in the area of contrast agents used in NMR imagery	10
2.1. Contrast agents	10
2.1.1. Contrast agents for sequence T1	10
2.1.2. Contrast agents for sequence T2	10
2.2. Contrast agents with Gadolinium	11
2.2.1. Omniscan	11
2.2.2. Multihance	11
2.2.3. State of art of researches in the area of contrast agents	11
2.3. Ferrite nanoparticles as contrast agents	11
2.4. Iron oxides as contrast agents	12
<b>Chapter 3</b> Magnetic nanoparticles and ferrofluids used as contrast agents	12
3.1. Methods of magnetic nanoparticles synthesis	12
3.1.1. Sol- gel method	12
3.1.2. Co-precipitation method	12
3.2. Methods for nanopowders structural characterization	12
3.2.1. X-rays diffraction	12
3.2.2. Transmission electron microscopy	13
3.2.3. Scanning electron microscopy	13
3.3. Methods for nanoparticle dispersion characterization	13
3.3.1. Nanosight LM20	13
3.4. Methods for magnetic characterization	14

3.4.1. Vibrating sample magnetometer	14
3.5. Synthesis and characterization of magnetic nanoparticles	14
3.5.1. Zn ferrite	14
3.5.2. Cobalt ferrite	14
3.5.3. Ni- doped zinc ferrite	15
3.5.4. Co- doped zinc ferrite	17
<b>Chapter 4</b> Experimental results of imagery	18
4.1. Methods for image generation and processing on phantoms	18
4.1.1. M-Fe <sub>2</sub> O <sub>3</sub> – type ferrites as contrast agents	18
4.1.2. Nanoparticles from Co <sub>x</sub> Zn <sub>1-x</sub> Fe <sub>2</sub> O <sub>4</sub> and Ni <sub>x</sub> Zn <sub>1-x</sub> Fe <sub>2</sub> O <sub>4</sub> series as contrast agents	20
4.1.3. Study of the Co <sub>x</sub> Zn <sub>1-x</sub> Fe <sub>2</sub> O <sub>4</sub> series as contrast agent	22
4.2. Methods for processing the NMR images of the nanoparticle dispersions	23
4.3. Characterization of dispersions in various liquids	23
4.3.1. Zinc ferrite	23
4.3.2. Multihance contrast agent	24
4.3.3. Omniscan contrast agent	25
<b>Chapter 5</b> Reasoning concerning the factors which influence the contrast	26
5.1. Study of the influence of ferrite nanoparticles synthesis method on the NMR images	27
5.2. Study of particle microstructure and mean size on the contrast of NMR images	28
5.3. Study of the influence of magnetization and mean particle size on the NMR images	28
5.4. Study of the susceptibility influence on the NMR images	28
General conclusions	29
Reference	31
List of ISI publications	33
List of non-ISI publications	34

The summary of the doctoral dissertation preserves the numbering of chapters, figures, tables and literature indications.

## Introduction

The nuclear magnetic resonance has known vast applications both in the research and the medical field, especially for establishing the diagnosis of some tumor pathologies. Given the fact that the tumor tissue and the pathologic tissue present a similar contrast in the medical magnetic resonance imagery, the solution was to use contrast agents. At first, the used contrast agents were based on gadolinium nanoparticles, more exactly gadolinium chelates. These are utilized due to their magnetic properties and biocompatibility with the human tissue. Another category of contrast agents used mainly in the USA is based on iron nanoparticles.

During the recent years, the research on the contrast agents has known a vast development, due also to the fact that the magnetic resonance imagery has more and more applications. The research theme concerning the nanoparticles with applications in medical imagery is nowadays of international importance and includes several research areas.

This work is structured in two parts: the first one approaches the magnetic resonance phenomenon and the present stage of the contrast agent research, while in the second part the personal contribution to the study of the nanoparticle influence on the contrast in medical magnetic resonance imagery are presented.

*Chapter 1* presents the basic principles of the magnetic resonance phenomenon. The phenomena of longitudinal and transversal relaxation of the magnetic moments subjected to a magnetic field, as well as the principles of NMR image formation are described here.

The first part of the *Chapter 2* presents the way in which the contrast agents acts on the proton magnetic moments, while in the second part is detailed a brief presentation of the present stage of researches dedicated to the nanoparticles used as contrast agents.

*Chapter 3* presents the methods for synthesizing the nanoparticles used in the study of their influence on the contrast in medical imagery. Here are presented the structural properties of the zinc, cobalt and nickel ferrites, as well as those of the  $\text{Co}_x\text{Zn}_{1-x}\text{Fe}_2\text{O}_4$  and  $\text{Ni}_x\text{Zn}_{1-x}\text{Fe}_2\text{O}_4$  series, with  $x$  ranging between 0 and 1, synthesized through the sol-gel self-combustion method.

*Chapter 4* presents details on the studies carried out on the dispersions of  $\text{ZnFe}_2\text{O}_4$ ,  $\text{NiFe}_2\text{O}_4$  and  $\text{CoFe}_2\text{O}_4$  nanoparticles and of the ferrite series with the general formula  $\text{Co}_x\text{Zn}_{1-x}\text{Fe}_2\text{O}_4$  and  $\text{Ni}_x\text{Zn}_{1-x}\text{Fe}_2\text{O}_4$  ( $x$  from 0 to 1) in agar phantom. The images obtained for these phantoms were also analyzed, in order to evaluate the contributions of magnetic moments of the ferrite nanoparticles on the longitudinal and transversal relaxation times. For the zinc ferrite synthesized through sol-gel self-combustion method a study was also performed meant to appreciate influence of the concentration on the contrast in medical imagery.

*Chapter 5* contains a comparative study of the contrast-related factors in the medical imagery. Comparisons between the synthesis methods, combustion agent, nanoparticles mean size and morphology, as well as the magnetic properties are presented.

The thesis ends with *General conclusions* of this study.

## **Chapter I. Basic principles of NMR**

### **1.1. Nuclear magnetic resonance**

The concept of magnetic resonance was used once discovering the nuclear spin (George Uhlenbeck and Samuel Goudsmith, 1925), followed by the study of the interaction between the spin and the magnetic field [1]. The magnetic resonance phenomenon was applied for the first time in physics and chemistry for the study of molecules [2]. The possibility of magnetic resonance utilization in the study of living tissue increased the interest in the development of a biomedical application, especially when it was noticed that the normal and abnormal tissues can be differentiated by means of the nuclear magnetic resonance. About four decades have past until the development of magnetic resonance installations, which have known a huge success. This started in 1922, when Otto Stern and Walter Gerlach experimentally noticed the electron spin quantification. In 1937, Isidor I. Rabi (Nobel Prize for Physics, 1944) noticed the nuclear magnetic resonance (NMR) phenomenon in the molecular beam.

## 1.2. Larmor precession

The Larmor's equations describe the magnetization precession in the magnetization process and are deduced from the classical electromagnetism theory. Making use of the magnetic moment, the torsion moment ( $T$ ) is given by the vector product between the magnetic moment ( $\mu$ ) and the applied magnetic field ( $B$ ) [3].

## 1.3. Relaxation times. Bloch's equations

### 1.3.1. Relaxation time $T1$

The balance magnetization ( $M$ ) is obtained when the magnetic vector is aligned along the applied magnetic field  $B'_o$ . If the system is acted upon by a magnetic field in the form of a radiofrequency impulse oriented under an angle of  $90^\circ$ , the magnetization  $M_z$  decreases to zero. The energy of the RF impulse must be bigger or equal to the difference of energy between the two spin energy states. The necessary time for the magnetization  $M_z$  to come back to the balance value is called time of spin- lattice relaxation or longitudinal relaxation time ( $T1$ ).

### 1.3.2. Relaxation time $T2$ .

After the RF impulse stops, the reverse phenomenon occurs, i.e. the transversal magnetization  $M_{xy}$  quickly decreases down to the balance value, being characterized by the transversal relaxation time  $T2$ , or spin-spin relaxation time.

## 1.4. Bloch equation

Until now, the interactions between the spin and its surrounding medium were not taken into account. In practice, it is necessary to take also into consideration the internal magnetic and electric fields caused by these interactions, as these can induce additional magnetization movements. This problem was studied by Bloch [4]. He proposed a set of equations that describe the evolution of the spin system.

## 1.5. Fourier Transform

The Fourier transform contains information about the real and the imaginary part for a well-defined phase. To shorten the time in the Fourier method, one proceeds to the scanning of half of the  $k$  space and then to the reconstruction of the other half, using the Hermitiene symmetry of the Fourier transform for the NMR signal,  $S(-k) = S^*(k)$ .

## 1.6. Image generation in the magnetic resonance imagery

For the acquisition of a MNR imagine, a small slice of the sample is excited. This can be done by simultaneously applying a magnetic field gradient and a selective impulse. The amplitude modulation in time is necessary to excite a limited section of the frequency spectrum. In the presence of a magnetic field, such an impulse will only excite a narrow section of the sample (we shall use the name of *slice* for the small section of the scanned sample). The slice thickness is proportional with the spectrum width. This effect can be noticed for the spatial variation of the magnetization after the application of a rectangular impulse during the time interval  $t_h$  in the presence of the gradient on the  $z$  axis,  $G_z$ .

## 1.7. Space $k$

The space  $k$  is a special concept in the NMR imagery technique, being used for data acquisition, reconstruction and visualization. The  $k$  space can be defined as an abstract platform on which the data are acquired, positioned and then converted in image. The space  $k$  must be filled-up with all the data before the image is reconstructed [5].

## 1.8. Artifacts in magnetic resonance imagery

The artifacts are noises overlapped on the spin relaxation signal and they can affect the obtain image. The artifacts depend on several factors, such as the artifacts due to patient and the artifacts due to the technique. The artifacts due to the patient are strictly

produced by his voluntary movements or by involuntary motions of the patient internal organs. The technique-generated artifacts arise from inadequate selection of the scanning parameters and/or the NMR installation failures [6].

## **1.9. NMR equipment used in medical diagnosis**

The installation of nuclear magnetic resonance consists in the following components: the magnet, the coil system that creates the magnetic field gradients, the detection systems (radiofrequency antennas), the reception system and the computer [7].

### **Chapter 2. State of art of the researches in the field of contrast agents used in NMR imagery**

#### **2.1. Contrast agents**

The contrast agents play an important role in the medical nuclear magnetic resonance imagery. The contrast products are mainly used to increase the contrast of the NMR images. At this moment there are several types of contrast agents in use: embedded in the extra cellular fluid (ECF), intravenous agents, and agents specific for certain tissues or organs.

##### ***2.1.1. Contrast agents for sequence T1***

The contrast agents used for the sequence T1 are generally paramagnetic metallic ions. At this moment, the mostly used paramagnetic ion is that of gadolinium (Gd). This possesses 7 unpaired electrons, which results in a big magnetic moment for each particle. The metallic ions  $Mn^{2+}$  and  $Fe^{2+}$  present a good contrast in the sequence T1, because they also have big magnetic moments [8].

##### ***2.1.2. Contrast agents for sequence T2***

The superparamagnetic or ferromagnetic substances induce magnetic field inhomogeneities which accelerate the proton phase difference, thus diminishing the relaxation time T2. It is often much

easier to influence the decrease of the spin-spin relaxation time (T<sub>2</sub>) using superparamagnetic agents. Part of these contrast substances includes iron oxide nanoparticles, namely magnetite (Fe<sub>3</sub>O<sub>4</sub>) or maghemite (γ-Fe<sub>2</sub>O<sub>3</sub>), with the average diameter of 5÷50 nm.

## **2.2. Contrast agents with Gadolinium**

Gadolinium is paramagnetic from a magnetically standpoint. The gadolinium chelates suspensions are used as contrast agents in the magnetic resonance imagery. The nanoparticles of Gd chelate have dimensions ranging between 5 and 100 nm and are dispersed in an injectable solution.

### ***2.2.1. Omniscan***

The contrast agent Omniscan contains 287 mg gadodiamide solved in an injectable solution and is generally used for the diagnosis of central nervous system tumors.

### ***2.2.2. Multihance***

Each milliliter of Multihance contrast agent contains 0.529 g of gadobenate dimeglumine solved in an injectable solution.

### ***2.2.3. State of art of the researches in contrast agent area***

Numerous papers, especially those published in magazines specialized in medicine, describe the importance of contrast agents in the diagnosis of various tumors or vascular lesions, even of millimeter size [9].

## **2.3. Ferrite nanoparticles as contrast agents**

The tendency in the medical area is to permanently develop medical equipment and accessories for a better visualization of anatomic regions, tumors and their infiltrates. A new range of contrast agents that are now investigated and developed are the ferrites.

## **2.4. Iron oxides as contrast agents**

The studied contrast agents based on gadolinium, ferrites and iron oxides have an effect on the relaxation time, which confirms that they can be used in the NMR technique. In order to be used as contrast agents, these substances must pass the tests of biocompatibility with the human organism. One of the techniques that make them biocompatible consists in covering them in polymers. Despite their high toxicity, some ferrites can thus be accepted by the human body. All the above described studies were performed in laboratories using NMR installations with high intensities of the magnetic field and by diluting in water different amounts of nanoparticles.

## **Chapter 3. Magnetic nanoparticles and ferrofluids used as contrast agents**

### **3.1. Methods of magnetic nanoparticle synthesis**

#### ***3.1.1. Sol- gel method***

The sol-gel synthesis method is used most often in the oxide metallic nanostructure synthesis. In the sol-gel synthesis, besides the physical and chemical processes, there other associated phenomena, such as hydrolysis, polymerization, grafting, condensation, drying and densification [10].

#### ***3.1.2. Co-precipitation method***

The co-precipitation method is the mostly used method in the synthesis of iron oxide ( $\text{Fe}_3\text{O}_4$  or  $\gamma\text{-Fe}_2\text{O}_3$ ) from the aqueous salt solution of  $\text{Fe}^{2+}/\text{Fe}^{3+}$ , with the addition of an alkali. The co-precipitation is also used in medicine to bind an antigen with an antigen-antibody complex [11].

### **3.2. Methods of nanopowder structural characterization**

#### ***3.2.1. X-rays diffraction***

The X-rays diffraction is a nondestructive technique used to determine the structural properties: lattice spacing, grain

dimension, phase composition. By means of this method one can also get information about the crystalline phase or atomic arrangement and one can measure the thickness of thin films or multilayered structures [12].

### ***3.2.2. Transmission electron microscopy (TEM)***

The transmission electron microscopy (TEM) offers data on the structural and ultrastructural properties of the solid internal structure that are impossible to be seen with an optical microscope.

### ***3.2.3. Scanning electron microscopy***

By means of the scanning electron microscopy one can analyze large scale samples, of the order of millimeters. The samples must be electrically conducting; if they are not electrically conducting, they will get electrostatically charged during the scanning process, generating a negative potential [13].

## **3.3. Methods of nanoparticle dispersion characterization**

### ***3.3.1. Nanosight LM20***

When investigating the nanoparticle dimensions, the team from NanoSight developed a unique instrument which allows following the Brownian motion of the particles in a liquid suspension. This technique is an alternative to the DLS (Dynamic Light Scattering) technique. The technique for the analysis of the moving nanoparticles (NTA- Nanoparticle Tracking Analysis) is a direct method for nanoparticles direct visualization and analysis in real time. The nanoparticle Brownian motion is analyzed by means of a microscope illuminated with a laser beam (30 mW, 635 nm), equipped with a CCD camera. By means of the dedicated software, one can analyze each particle apart, which allows determining the nanoparticle dimension (hydrodynamic diameter).

### 3.4. Methods of magnetic characterization

#### 3.4.1. Vibrating sample magnetometer

The vibrating sample magnetometer (VSM) was developed by S. Fonner in 1956. By means of this installation, one can measure the magnetic properties of materials.

### 3.5. Synthesis and characterization of magnetic nanoparticles

#### 3.5.1. Zinc ferrite

The zinc ferrite nanoparticles, with the general formula  $\text{ZnFe}_2\text{O}_4$ , was synthesized through the sol-gel self-combustion method in the Laboratory of the Chemistry Faculty of the “Al. Ioan Cuza” University of Iassy, under the direction of PhD Prof. Nicolae Palamaru. In this connection, the metallic nitrates were used as precursors, while the citric acid was used as combustion chelating agent.

By analyzing the XRD diffractograms of the sample heat treated at  $900^\circ\text{C}$  (Fig. 3.7), it follows that the zinc ferrite is of spinel type.

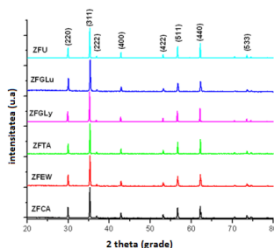


**Fig. 3.7.** XRD diffractograms of the sample heat treated at  $900^\circ\text{C}$  [14]

#### 3.5.2. Cobalt ferrite

The cobalt ferrite nanoparticles, with the general formula  $\text{CoFe}_2\text{O}_4$ , were synthesized through the process of low temperature combustion in the Laboratory of the Chemistry Faculty of the “Al. Ioan Cuza” University of Iassy, under the direction of PhD Prof. Nicolae Palamaru.

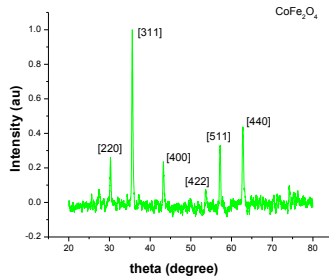


**Fig. 3.9.** XRD diffractograms for cobalt ferrite treated at the temperature of 850°C [16]

The lattice parameter obtained from the XRD diffractograms, Fig. 3.9, for the powders of Co ferrite is  $a = 8.3802 \text{ \AA}$ , which agrees with the specialized literature [15]. As the result of structure measurements, it was found that the cobalt ferrite synthesized through combustion presents an fcc cubic spinel structure. The magnetic measurements show that the cobalt ferrite possesses magnetic properties which recommend it for utilization in practical applications (Fig. 3.10). The heat treatment to which the sample was subjected resulted in the increase of the mean grain dimension and the decrease of the coercive force value.

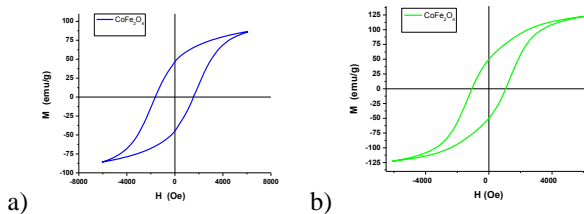


**Fig. 3.10.** Hysteresis loop for  $\text{CoFe}_2\text{O}_4$  calcined at the temperature of: a) 650°C and (b) 850°C [16]

### 3.5.3. Nickel-doped zinc ferrite

The nickel-doped zinc ferrite was obtained through the sol-gel self-combustion method, using the tartaric acid as combustion agent, in the Laboratory of the Chemistry Faculty of the “Al. Ioan

Cuza” University of Iassy, under the direction of PhD Prof. Nicolae Palamaru. The general formula of the nickel-doped zinc ferrite is:  $Ni_xZn_{1-x}Fe_2O_4$  ( $x=0; 0.2; 0.4; 0.6; 0.8; 1$ ), noted with ZF, NZF0.2, NZF0.4, NZF0.6, NZF0.8, NF, where ZF is  $ZnFe_2O_4$ , and NF is  $NiFe_2O_4$  [17].

The XRD diffractograms for the Ni-Zn ferrite are presented in Fig. 3.11. From their analysis one can notice that the highest peak is at  $2\theta= 35^\circ$ ; it can be found for the entire ferrite series and is assigned to the (311) index, which is typical for the spinel phase. All the peaks from the diffractograms were identified and they agree with the data base offered by the International Centre for Diffraction Data)[18].

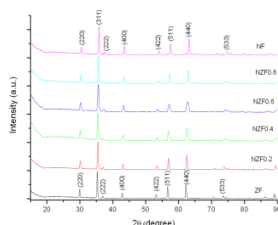


**Fig. 3.11.** XRD diffractograms for  $Ni_xZn_{1-x}Fe_2O_4$  treated at  $700^\circ C$  [17]

In Fig. 3.12. it can be observed the ZF sample is paramagnetic and with the increase of the Ni concentration, the magnetization increases up to 55 emu/g. This suggests that the samples are a blend of ferrimagnetic particles with their size exceeding the critical dimension, and particles smaller than the critical dimension, which behave superparamagnetically. One can notice a gradual improvement of the magnetic properties with the increase of the Ni ions concentration.

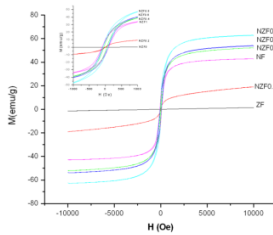


**Fig. 3.12.** Hysteresis loop at room temperature for  $Ni_xZn_{1-x}Fe_2O_4$  ferrite powders heat treated at the temperature of  $700^\circ C$  [17]

### 3.5.4. Cobalt doped zinc ferrite

The cobalt doped zinc ferrite was obtained through sol-gel combustion method, using the tartaric acid as combustion agent, in the Laboratory of the Chemistry Faculty of the “Al. Ioan Cuza” University of Iassy, under the direction of PhD Prof. Nicolae Palamaru. The general formula of the cobalt-doped zinc ferrite is:  $Ni_xZn_{1-x}Fe_2O_4$  ( $x=0; 0.2; 0.4; 0.6; 0.8, 1$ ) [19].

The XRD diffractograms revealed the formation of the pure spinel phase for all the samples. The most intense peak, characteristic for the spinel structure, was recorded at  $2\theta=35^\circ$ , Fig. 3.13. The shape of nanoparticles of cobalt substituted zinc ferrite is cubic [19].

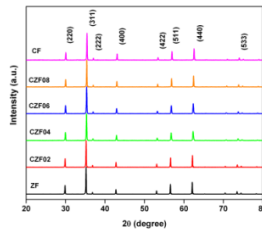


**Fig. 3.13.** XRD diffractograms for  $Co_xZn_{1-x}Fe_2O_4$  [8]

The variation of magnetization with magnetic field (maximum 10 kOe) for the samples from the CZF samples was

studied at room temperature and represented in the form of magnetization curves in Fig. 3.14. One can notice that the saturation magnetization increases with the increase of Co content in the Zn ferrite, and the passage to the paramagnetic (ZF, CZF02 samples) to the ferimagnetic behavior (CZF04, CZF06, CZF08, CF) occurs under the influence of magnetic cations  $\text{Fe}^{3+}$  and  $\text{Co}^{2+}$  from the B lattice, which contribute to the total magnetization of the studied samples. The small dimensions of nanoparticles and the existence of a large number of single domains can result in the decrease of the saturation magnetization, this decrease being amplified by the motion of the domain walls [19].

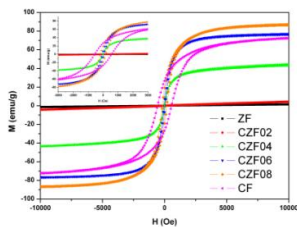


Fig. 3.14. Magnetization curves for the samples of CZF series

## Chapter IV. Experimental results of imagery

### 4.1. Methods for image generation and processing on phantoms

#### 4.1.1. Ferrites of $M\text{Fe}_2\text{O}_4$ series ( $M = \text{Co}, \text{Zn}, \text{Ni}$ ) as contrast agents

The present study proposed the determination of the influence of nanoparticles of zinc ferrite ( $\text{ZnFe}_2\text{O}_4$ ), cobalt ferrite ( $\text{CoFe}_2\text{O}_4$ ) and nickel ferrite ( $\text{NiFe}_2\text{O}_4$ ) on the contrast of RMN medical images. These nanoparticles were synthesized through the sol-gel self-combustion method in the Laboratory of the Chemistry Faculty of the “Al. Ioan Cuza” University of Iassy, under the direction of PhD Prof. Nicolae Palamaru. The results were compared with those obtained in the case of utilization of two contrast agents already existing on the medicine market from Romania (Omniscan® and Multihance®).

With this aim in view, a number of six agar-based phantoms were executed, which simulate the human tissue and whose image in the magnetic resonance imagery is comparable with that of the human tissue. For phantom realization we used 900 ml distilled water, 0.28 g nickel chloride ( $\text{NiCl}_2$ ), 30 g agar, 5 g sodium chloride ( $\text{NaCl}$ ) and 0.25 g azide. The sodium chloride is added to increase the phantom conductivity [20].

The composition realized from the above materials was divided in six equal parts of 160 ml each. In the first three phantoms we introduced 0.5 g ferrite ( $\text{CoFe}_2\text{O}_4$ ,  $\text{ZnFe}_2\text{O}_4$  and  $\text{NiFe}_2\text{O}_4$ ). In other two phantoms we introduced 1 ml of contrast substance, i.e. Omniscan and Multihance respectively, which contain 0.5 g gadolinium. These contrast agents consist of nanoparticles of gadolinium chelates (Gd): gadodiamide ( $\text{GdDTPA-BMA}$ ) and gadobenic acid. The last phantom represented the witness sample, containing only agar.

The phantoms were scanned at a NMR installation equipped with a permanent magnet with the field intensity of 0.4 T, using the head coil. The images during the T1 and T2 sequences were obtained as the result of phantom scanning at the NMR installation. Fig. 4.6, a presents the axial images in the T1 sequence obtained by scanning the agar phantoms with dispersions of nanoparticles of Zn, Co and Ni ferrites. Fig. 4.6,b presents the axial images of these phantoms obtained in the T2 sequence.

From the analysis of the above images, one can notice that the phantoms that contain paramagnetic contrast substance (Gd) presents a positive contrast in the T1 sequence (Fig. 4.5), which is confirmed by the results presented in literature. Besides these, the phantoms with Ni and Co ferrites present a moderate contrast during the T1 sequence, close to those based on Gd. It is thus proved that the Ni and Co ferrites can be a solution for the contrast agent for the T1 sequences, by increasing the nanoparticle concentration or by using nanoparticles with dimensions ranging between 50 and 150 nm. The influence of the contrast on the magnetic resonance imagery is given by the nanoparticle magnetic properties too. In order to use them in magnetic resonance medical imagery, they need to be biocompatibilized by covering them with polymers.

The Zn ferrite shows no contrast in the T1 sequence, its image being dark. Yet, it presents an intense signal in the T2

sequence, which has as an effect the shortening of relaxation time T2, Fig. 4.6, b). The cobalt and nickel ferrite, as well as the contrast agents with Gd, present a dark image in the T2 sequence.

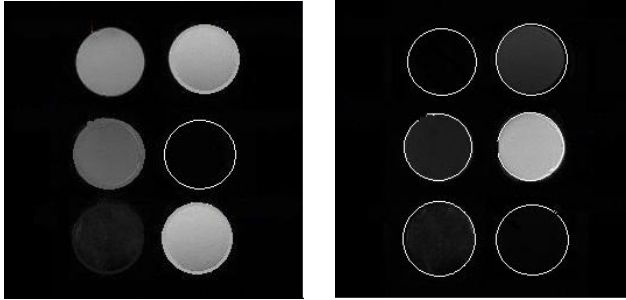


**Fig. 4.6.** Representation of the NMR images: a) image in T1 sequence; b) image in T2 sequence

#### ***4.1.2. Nanoparticles from the series $\text{Co}_x\text{Zn}_{1-x}\text{Fe}_2\text{O}_4$ and $\text{Ni}_x\text{Zn}_{1-x}\text{Fe}_2\text{O}_4$ ( $x=0; 0.2; 0.4; 0.6; 0.8; 1$ ) as contrast agents***

We proposed to study the influence of nanoparticles of zinc ferrite doped with nickel and cobalt of various concentrations, on the contrast of NMR images. We meant to analyze the contribution of cobalt and nickel ions to the contrast in the magnetic resonance imagery when these substitute the zinc ions.

In the study of the influence of  $\text{Co}_x\text{Zn}_{1-x}\text{Fe}_2\text{O}_4$  ( $x=0; 0.2; 0.4; 0.6; 0.8; 1$ ) and  $\text{Ni}_x\text{Zn}_{1-x}\text{Fe}_2\text{O}_4$  ferrites on the NMR image contrast, we resorted to the realization of agar phantoms in which ferrite nanoparticles and commercial contrast agents (used as witnesses) were dispersed. The zinc ferrites doped with cobalt/nickel were synthesized through the sol-gel self-combustion method in the Laboratory of the Chemistry Faculty of the “Al. Ioan Cuza” University of Iassy, under the direction of PhD Prof. Nicolae Palamaru (the method of synthesis and characterization is described in Chapter III).

For phantom realization, we used 2500 ml distilled water, 75 g agar, 12.5 g sodium chloride (NaCl) and 0.625 g azide. The solution obtained by mixing these materials was divided in 15 equal parts of 160 ml each. In two of the samples we introduced 0.1 ml

contrast agents Omniscan and Multihance respectively, used in the NMR imagery. In other 16 samples we introduced 0.5 g of ferrite from the above series. The last phantom was considered as witness, being made of agar without nanoparticle or contrast substance dispersions.

The samples were scanned using the same NMR installation, as for the phantoms with ferrites of the form  $MFe_2O_4$  (M= Co, Zn, Ni).

From the analysis of the images from Fig. 4.13 a) and b), one can notice that in the T1 sequence the phantoms with contrast agents Omniscan and Multihance present a positive contrast, while in the T2 sequence they do not show a positive contrast, these data agreeing with the data from literature [20]. The phantom that contains the  $Co_xZn_{1-x}Fe_2O_4$  ferrite ( $x=0$ ) presents a positive contrast in the T2 sequence. The images of the phantom in which ferrite particles with  $x=0.2$  were dispersed show a moderate positive contrast in the T2 sequence. The signal intensity in the T2 sequence significantly decreases with the increase of the cobalt concentration. As we have seen both in sub-chapter 4.1 and in the experimental data produced by other research teams, the zinc ferrite influences the relaxation time T2, while the cobalt ferrite influences the relaxation time T1. As for the Co-doped Zn ferrite, it shows no influence on the relaxation times T1 and T2, especially for concentrations values  $x > 0.6$ .

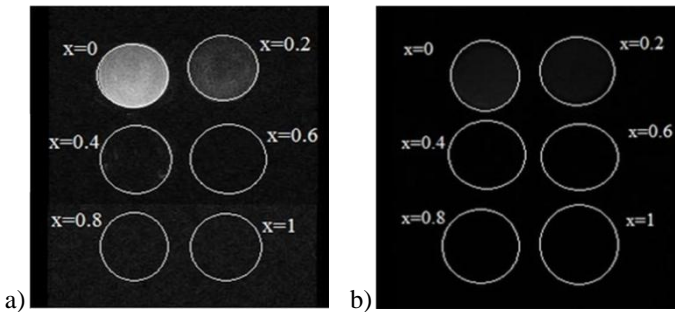


**Fig. 4.13.** Images of phantoms with dispersion of nanoparticles from the ferrite series, scanned at a NMR installation of 0.4 T; a) T2 sequence; b) T1 sequence

### 4.1.3. Study of the $\text{Co}_x\text{Zn}_{1-x}\text{Fe}_2\text{O}_4$ series as contrast agent

The next step consisted in the study of the influence of nanoparticles of ferrite with the chemical formula  $\text{Co}_x\text{Zn}_{1-x}\text{Fe}_2\text{O}_4$  ( $x = 0; 0.2; 0.4; 0.6; 0.8; 1$ ) synthesized through co-precipitation, on the contrast of the images obtained in medical NMR imagery. The ferrite series was synthesized within the Department of Chemistry-Physics from the University of Saarland, Germany. The results were compared with the results obtained for the zinc ferrite with the same properties, but synthesized through sol-gel self-combustion method. The phantom preparation was identical with that presented above, including the concentrations of ferrite and contrast agent. The agar phantoms containing nanoparticles of  $\text{Co}_x\text{Zn}_{1-x}\text{Fe}_2\text{O}_4$  ferrite ( $x = 0; 0.2; 0.4; 0.6; 0.8; 1$ ), Multihance (Braco), Omniscan (GE) and witness (agar phantom) were scanned at the same NMR installation (Hitachi, Japan), using the same scanning parameters and geometry. The images obtained in the T1 and T2 sequences are presented in Fig. 4.2.1.

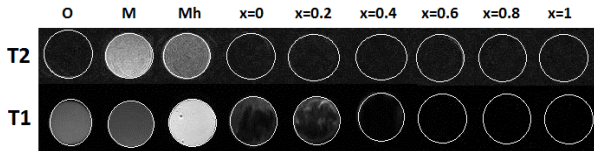


**Fig. 4.21.** Images scanned with NMR installation for the T1 and T2 sequences [22]

In Fig. 4.21 the image obtained with Omniscan contrast agent was marked with O, the witness was marked with M, and the phantom noted with Mh contained Multihance. For the  $\text{Co}_x\text{Zn}_{1-x}\text{Fe}_2\text{O}_4$  the phantoms were marked according to the amount of doping agent. One can notice that the phantoms containing Omniscan or Multihance present a positive contrast in the T1 sequence, which agrees with the data from literature [23] and with those obtained for cobalt-doped zinc ferrite, synthesized through sol-gel self-combustion method. The witness sample which simulates the healthy tissue presents a different signal for the two sequences [24].

## 4.2. Methods for processing the NMR images of nanoparticles dispersions

We proposed to accomplish a study of the ferrite nanoparticle dispersions in aqueous solutions. For this goal, we used the zinc ferrite that determines the contrast in the T2 sequence, and Multihance contrast agent, which is based on gadolinium chelates and presents a good contrast in the T1 sequence. For dispersion preparation we used different amounts of zinc ferrite: 0.003g, 0.006g, 0.015g, 0.03g, 0.06g, 0.15g and 0.3g, these being dispersed in 10 ml ultra pure de-ionized water. As in the case of contrast agent, concentrations of 0.03 ml, 0.06 ml and 0.1 ml were dispersed in de-ionized water. A flask containing only de-ionized water was used as witness.

The flasks with dilutions prepared in this way were scanned at the NMR installation Aperto 0.4 T, using the same scanning parameters as for the others phantoms. The resulted images are presented in Fig. 4.22.

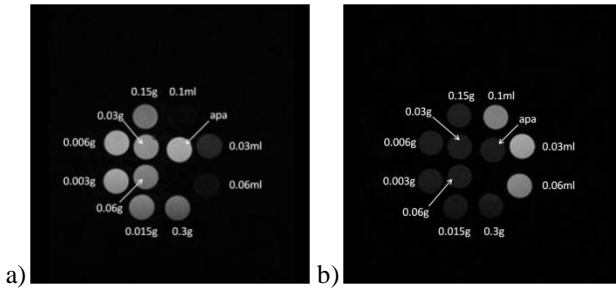


**Fig. 4.22.** Images of phantoms containing suspensions of zinc ferrite and Multihance: a) T2 sequence; b) T1 sequence

## 4.3. Characteristics of dispersions in different liquids

### 4.3.1. Zinc ferrite

The average nanoparticle dimension was determined through optical method by means of the analyzer (microscope) of nanoparticles motion within the liquid, Nanosight LM 20 from the Laboratory of Solid State Physics.

Determination of the mean size of particles of zinc ferrite synthesized through sol-gel self-combustion method [22] was performed by dispersing the ferrite in normal saline solution and introducing the suspension in the working case. The experiment was carried out at a temperature of 26.15°C. The suspension viscosity during the determination was of 0.87 cP; the nanoparticle concentration was determined as being equal to  $11.59 \cdot 10^8$  particles/ml. The time interval for nanoparticle registration was of 60 seconds, their mean speed being of 2025 nm/s. The above values were determined from a total number of 1550 particles, for which the complete motion was detected and determined. Fig. 4.25 presents the histogram of the distribution of the zinc ferrite nanoparticles dimensions. One can learn that the mean size of the zinc ferrite nanoparticles is 61 nm, which agrees with the values obtained from TEM [22].

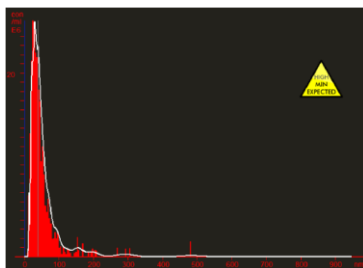


**Fig. 4.25.** Representation of the histogram of the distribution of zinc ferrite nanoparticles according to their dimensions

#### **4.3.2. Multihance contrast agent**

The determination of the dimensions of the contrast agent Multihance nanoparticles was performed by means of the installation Nanosight LM 20. For this goal, a dilution was made from distilled water and Multihance at a ration of 2:1. The measurements were carried out at a temperature of 26.15°C. The dilution viscosity during the determinations was of 0.87 cP, while data acquisition times were  $t = 10$  and  $t = 100$  s. Fig. 4.26 presents the concentration of nanoparticles of gadolinium chelate in terms of

their dimensions, for various acquisition times. By analyzing the graphics from Fig. 4.25, one can notice that, with the increase of the acquisition time from 10 to 100 s, the concentration of gadolinium nanoparticles from the suspension diminishes from  $8 \cdot 10^6$  particles/ml to  $4 \cdot 10^6$  particles/ml. For the acquisition time of 10 s, the mean dimension of particles is almost equal to 40 nm, while at a time of 100 s, the mean particle dimension is of 34 nm. The long acquisition times also reveal the big dimensions of particles (900 nm), generally due to particle agglomerations. Since the microscope software accomplishes a time mediation of nanoparticle dimensions, one can learn that for long times of recording of the nanoparticles motions in suspension, their dimension decreases.

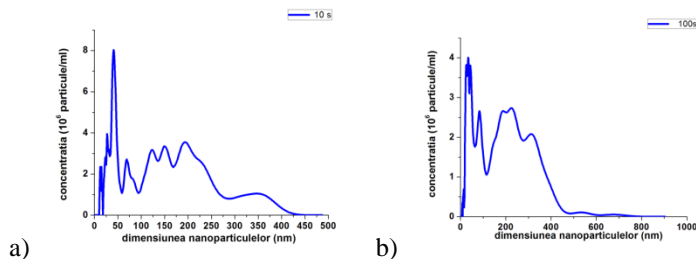


**Fig. 4.26.** Graphical representation of nanoparticle concentration in suspension as function of their dimension for various acquisition times: a) 10 s; b) 100 s.

#### 4.3.3. Omniscan contrast agent

The dimensions of the Omniscan contrast agent nanoparticles were determined under the same conditions as for Multihance (Fig. 4.28). In this case too it was established that, with the increase of the acquisition time from 10 s to 100 s, the concentration of gadolinium nanoparticles in suspension decreases from  $7.5 \cdot 10^6$  particles/ml to  $3 \cdot 10^6$  particles/ml.

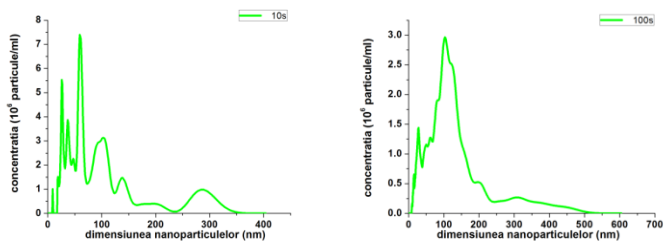


**Fig. 4.28.** Graphical representation of the nanoparticles concentration from suspension in terms of their dimensions for different acquisition times: a) 10 s; b) 100s

For the acquisition time  $t=10$ s, the first peak is visible at the mean particle size of 8 nm, followed by another peak corresponding to the dimension of 25 nm, while for  $t=100$  s, the mean particle size is of 25 nm. The next values of nanoparticle dimensions are only multiples of 25 (50 nm, 75 nm, 100 nm), these being spontaneous agglomeration of nanoparticles with the dimensions of 25 nm.

### Chapter V. Reasoning concerning the factors which influence the contrast

The image contrast is influenced by the technical parameters of image acquisition and by the contrast agents. The technical parameters of image acquisition resulting in contrast modifications are: echo time, repetition time and signal to noise ratio. The contrast agents improve the contrast of the NMR images if these are administrated correctly (each agent must be administrated according to the corresponding affections and organs) and in optimum concentration.

In this chapter we present the results of the comparative study of the properties of the ferrites utilized in our experiments as contrast agents in medical magnetic resonance imagery. The influence of the synthesis method, the combustion agent and the mean particle size on nanoparticle magnetization and susceptibility

were analyzed, trying to correlate these factors with the manner in which they influence the NMR image contrast.

### **5.1. Study on the influence of the ferrite nanoparticle synthesis method on the NMR images.**

In Chapter IV we discussed the influence of the ferrite nanoparticles synthesized through various methods, on the contrast of medical NMR images. Part of these nanoparticles were synthesized through sol-gel self-combustion method, by favor of the, research team from the Faculty of Chemistry from the “Al. I. Cuza” University of Iassy, while other ferrites were synthesized through co-precipitation method, within the Physics-Chemistry Department from the University of Saarland, Germany.

From the analysis of the images of agar phantoms with ferrite nanoparticles dispersions presented in Chapter IV, it follows that the synthesis method represents an important factor of influence on nanoparticle structural and magnetic properties, which determines accordingly its utilization in medical NMR imagery. The nanoparticles of zinc, cobalt and nickel ferrites, as well as nickel/cobalt-doped zinc ferrites, synthesized through the sol-gel self-combustion method and dispersed in agar phantoms and then scanned with the NMR installation, brought significant contributions in the process of nuclear magnetic moment relaxation. For instance, the zinc ferrite presented a contrast in the T2 sequence, while the nickel and cobalt ferrites influenced the image contrast in the T1 sequence [25]. The nickel/cobalt-doped zinc ferrites, with the general formula  $\text{Ni}_x\text{Zn}_{1-x}\text{Fe}_2\text{O}_4$  and  $\text{Co}_x\text{Zn}_{1-x}\text{Fe}_2\text{O}_4$ , with  $x= 0, 0.2, 0.4, 0.6, 0.8, 1$ , influenced the contrast in the T2 sequence for  $x= 0$  and  $x= 0.2$ . With the increase of the content of nickel and cobalt which substitute Zn, it was noticed that they have no contribution in the process of nuclear magnetic moment relaxation and no influence on the contrast in the two sequences [26].

The ferrite synthesized through the co-precipitation method at the Physics-Chemistry Department from the University of Saarland, Germany were also dispersed in agar phantoms and scanned under the same experimental conditions, using the same NMR scanning parameters. It was found that they had no influence

on the nuclear magnetic moment relaxation and accordingly on the contrast of NMR images.

## **5.2. Study of particle microstructure and mean size on the contrast of NMR images**

Because the Zn ferrite determines a very good contrast of the NMR images in the T2 sequence, we tried to investigate the influence of the combustion agent on nanoparticle morphology [26]. The citric acid, egg-white, tartaric acid, glycine, glucose and urea were used as contrast agents.

A major contribution in the study of zinc ferrite as contrast agent is represented by the combustion agent. Out of the six combustion agents used to obtain zinc ferrite nanoparticles, the tartaric acid had a significant influence on the relaxation time. This combustion agent was also used in the synthesis of nickel and cobalt ferrites studied as contrast agents [25]. The zinc ferrite synthesized through sol-gel method, making use of egg-white as combustion agent, presented a weak contrast in the sequence T2- i.e. a minimum influence of the relaxation time T2. The other zinc ferrites for which glycine, glucose, urea and citric acid were used as combustion agents had no influence on the magnetic moment relaxation time.

## **5.3. Study of the influence of magnetization and mean particle size on the NMR images**

By comparing the mean dimensions of the nanoparticles dispersed in agar phantoms, with their influence on the contrast in medical NMR imagery, one can notice that the nanoparticles with dimensions ranging between 30 and 70 nm influenced the relaxation times T1 and T2; these were synthesized through sol-gel self-combustion method. In exchange, the nanoparticles with the dimensions ranging between 7- 20 nm, synthesized through co-precipitation method had no influence on the relaxation times.

## **5.4. Study of the susceptibility influence on the NMR images**

The effects of field inhomogeneities depend on field disturbance as compared to pixel dimensions. The susceptibility

effects are the result of intravoxel dephasing and to the off-resonance effects.

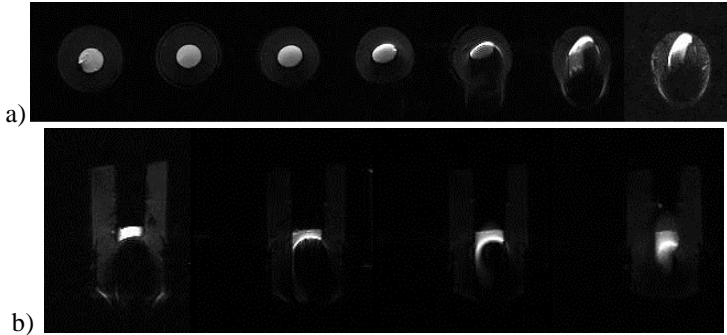


**Fig. 5.2.** Illustration of the effect of different susceptibility-intravoxel dephasing: a) T2 sequence - axial; b) T2 sequence - coronal

*Intravoxel dephasing*- the disturbance occurs on a relatively small distance as compared to voxel dimensions; the effect consists in the increase of voxel volume. In the case when the disturbance occurs on a distance higher than voxel dimension, the effect consists in recording the dephased signal as being constantly approximated with upward or downward displacement as compared to the reference value. This effect is also named off-resonance effect [28].

## GENERAL CONCLUSIONS

The main goal of this dissertation was to investigate the influence of the particles of spinel ferrites on the contrast in the medical magnetic resonance imagery. In this connection, the influence of the magnetic moments of the spinel ferrites on the longitudinal and transversal relaxation times was studied. As study materials we used nanoparticles of  $\text{ZnFe}_2\text{O}_4$ ,  $\text{NiFe}_2\text{O}_4$ ,  $\text{CoFe}_2\text{O}_4$ ,  $\text{Ni}_x\text{Zn}_{1-x}\text{Fe}_2\text{O}_4$  and  $\text{Co}_x\text{Zn}_{1-x}\text{Fe}_2\text{O}_4$ , as well as  $\text{Mn}_x\text{Fe}_{1-x}\text{Fe}_2\text{O}_4$ ,  $\text{Co}_x\text{Fe}_{1-x}\text{Fe}_2\text{O}_4$ ,  $\text{Zn}_x\text{Mn}_{1-x}\text{Fe}_2\text{O}_4$ .

Considering our goal, the first step consisted in the dispersion of nanoparticles of spinel ferrites in agar gels, and then their scanning at a NMR installation with a magnetic field of 0.4 T.

For comparison, we used contrast agents containing gadolinium chelates. These present a paramagnetic behavior and have the property to influence the transversal relaxation time. The zinc ferrite influenced the relaxation of hydronium magnetic moment and a positive contrast was revealed in the T2 sequence. The magnetic moments of the cobalt and nickel ferrites influenced the transversal relaxation time, showing a contrast in the T1 sequence.

The nanoparticles from the series  $\text{Ni}_x\text{Zn}_{1-x}\text{Fe}_2\text{O}_4$  and  $\text{Co}_x\text{Zn}_{1-x}\text{Fe}_2\text{O}_4$  (with  $x= 0, 0.2, 0.4, 0.6, 0.8$  and  $1$ ) synthesized through the sol-gel self-combustion method showed a paramagnetic behavior for  $x= 0$  and  $x= 0.2$ , and a ferrimagnetic behavior for  $x= 0.4, 0.6, 0.8$  and  $1$ . The nanoparticles with paramagnetic behavior contributed to a slower relaxation of the magnetic moments, resulting in a longer longitudinal relaxation time and implicitly, a contrast in the T2 sequence. For the ferrite nanoparticles with ferrimagnetic behavior, the values of the transversal relaxation times are very small. They presented no contrast in the T1 sequence.

The nanoparticles synthesized through co-precipitation method, with dimensions ranging between 8-18 nm and dispersed in agar gels, brought no contribution to the increase of the values of longitudinal and transversal relaxation times, the NMR signal having a very weak intensity.

A second step in our study consisted in the analysis of the dispersions of zinc ferrite and the contrast agent Multihance for various concentrations. Dilutions were made in ultra pure de-ionized water and scanned at the NMR installation.

The nanoparticle dispersion in aqueous solutions rendered evident that the magnetic moments of the zinc ferrites influence the longitudinal relaxation time. This influence is directly proportional with the increase of the number of magnetic moments from the ferrite concentration. For high concentration of zinc ferrite in aqueous solutions (0.06- 0.3 g), a constant plateau of the grey shade level is recorded- a small number of magnetic moments presents a big influence on the longitudinal relaxation time. For the Multihance contrast agent, one can remark a large transversal relaxation time with the increase of the concentration of gadolinium magnetic moments, this increase of the relaxation time being proportional with the concentration of contrast agent magnetic moments.

In the third part of our research, we dealt with the analysis of the influence of the synthesis method, the mean particle dimensions and their magnetization.

The nanoparticles synthesized through the co-precipitation method and sol-gel self-combustion method, have an influence on the medical imagery contrast. The nanoparticles synthesized through the co-precipitation method, with mean crystallite size ranging between 8 and 18 nm have no influence on the longitudinal or transversal relaxation times. The nanoparticles synthesized through sol-gel self-combustion method, with dimensions up to 70 nm, influence the longitudinal and transversal relaxation times. The synthesis method, the dimensions and magnetic properties of the utilized nanoparticles have a significant influence on the medical imagery contrast.

The combustion agent also presented an important role in the study of the medical imagery contrast. For zinc ferrite synthesis we used citric acid, egg-white, tartaric acid, glycine, glucose and urea as contrast agents. The relaxation time T<sub>2</sub> was influenced by the zinc ferrite synthesized with tartaric acid and white-egg, these presenting a paramagnetic behavior under the action of a magnetic field.

The magnetic susceptibility constitutes an important factor in medical imagery, given the appearance of susceptibility effects when two close zones presents large susceptibility variations. These are translated through artifacts and can be revealed by the zones without signal on the NMR image or distortions of the examined regions. These artifacts can not be removed, but their effect on the image can be diminished.

## **Bibliografie**

- [1] J. M. D. Coey, *Magnetism and magnetic materials*, Cambridge University Press, The Edinburgh Building, Cambridge CB2 8RU, UK, 2009.
- [2] K. Krzysztof, M. Kretowski, *Virtual magnetic resonance imagin – parallel implementation in a cluster computing environment*, Biocybernetics and Biomedical Engineering, 29(3) (2009) 31-46.
- [3] G. E. Sarty, *MRI physics for life science researchers*, University of Saskatchewan, Canada, 2005.

- [4] K. Kopinga, *Basics of magnetic resonance imaging*, IRTG wokshop, 2004.
- [5] A. O. Rodriguez, *Principles of magnetic resonances imaging*, Revista mexicana de fisica, 50(3) (2004) 272-286.
- [6] T. B. Smith, K. S. Nayak, *MRI artifacts and correction strategies*, Imaging Med. 2(4) (2010) 445-457.
- [7] S. Clare, *Functional MRI: Methods and applications*, University of Nottingham, Anglia 1997.
- [8] Carlos Barcena, Amandeep K. Sra, Girija S. Chaubey, Chalermchai Khemtong, J. Ping Liub and Jinming Gao, *Zinc ferrite nanoparticle as MRI contrast agents*, ChemComm, pp. 2224-2226, 2008.
- [9] Alan Jasanoff, *MRI contrast agents for functional molecular imaging of brain activity*, Current opinion in neurobiology, 2007;
- [10] S. Laurent, D. Forge, M. Port, A. Roch, C. Robic, L. V. Elst, R. N. Muller, *Magnetic iron oxide nanoparticles: synthesis, stabilization, vectorization, physicochemical characterizations and biological applications*, Chem. Rev. 108(2008) 2064-2110.
- [11] An-Hui Lu, E. L. Salabas, F. Schuth, *Magnetic nanoparticle: synthesis, protection, functionalization and applicaton*, Angew. Chem. Int. Ed. (46)(2007) 1222-1244.
- [12] J. R. Connolly, *Introduction to X-ray power diffraction*, Spring, 2012.
- [13] V. Pop, I. Chicinas, N. Jumate, *Fizica materialelor. Metode experimentale*. Presa Universitara Clujeana, 2001.
- [14] T. Slătineanu, E. Diana, V. Nica, V. Oancea, O. F. Caltun, A. R. Iordan, M. N. Palamaru, *The influence of chelating-combustion agents on the structural characteristics and magnetic properties of zinc ferrite*, Cent. Eur. J. Chem. 10 (2012) 1799-1807;
- [15] A.S. Parakash, A. M. Khadar, *Journal of Materials Synthesis and Processing*, 10(3) (2002);
- [16] M. N. Palamaru, A. R. Iordan, C. D. Aruxandei, I. A. Gorodea, I.A. Perianu, I. Dumitru, M. Feder, O. F. Călțun, *The synthesis of doped manganese cobalt ferrites by auto combustion tehniqe*, Journal of optoelectronics and advanced materials, 7 (10) (2008) 1853-1856;
- [17] T. Slătineanu, A. R. Iordan, M. N. Palamaru, O.F. Călțun, V. Gafton, L. Leontie, *Synthesis and characterization of nanocrystalline Zn ferrites substituted with Ni*, Materials research bulletin, 46 (2011) 1455-1460.
- [18] Bază de date 52-0278 ICDD, 2002 JCPDS;
- [19] T. Slătineanu, A. R. Iordan, V. Oancea, M. Palamaru, I. Dumitru, C. P. Constantin, O. F. Călțun, *Magnetic and dielectric properties of Co-Zn ferrite*, Materials Science and Engineering: B, 178(16) (2013) 1040-1047.
- [20] G. J. Strijkers ș.a., *Anti-cancer agents in medicinal chemistry*, pp. 291-305, 2007.

- [21] S. Aime, C. Cabella, S. Colombatto, C. Geninatti, E. Gianolio, F. Muggioni, *Insights into the use of paramagnetic Gd(III) complexes in MR-molecular imaging investigations*. *J. Magn. Reson. Imaging*, 2002.
- [22] A. Doagă, A. M. Cojocariu, C. P. Constantin, R. Hempelmann, O. F. Călțun, *Magnetic nanoparticles for medical applications: progress and challenges*, AIP Proceed – trimis spre publicare.
- [23] D. H. Carr, J. Brown, G. M. Bydder, R. E. Steiner, H. J. Weinmann, U. Speck, A. S. Hall, I. R. Young, Gadolinium-DTPA as a *contrast Agent in MRI: initial clinical experience in 20 patients*, *AJR* 143(1984) 215-224;
- [24] B. Ebrahimi, S. D. Swanson, B. Masadegh, T. E. Chupp, *A perfusion phantom for quantitative medical imaging*, *Physics of Medical Imaging*, 6913 (2008).
- [25] C. P. Constantin, A. Doaga, A. M. Cojocariu, I. Dumitru, O. F. Caltun, *Improved contrast agents for magnetic nuclear resonance medical imaging*, *Journal of Advanced Research in Physics* 2(2) (2011) 011106.
- [26] C. P. Constantin, T. Slătineanu, M. Palamaru, A. Iordan, O. F. Călțun, *Co<sub>x</sub>Zn<sub>x-1</sub>Fe<sub>2</sub>O<sub>4</sub> nanoparticles ferrite series as magnetic resonance imaging contrast agents*, *Digest Journal of Nanomaterial and Biostructures*, 7(4) (2012) 1793-1798.
- [27] T. Slătineanu, E. Diana, V. Nica, V. Oancea, O. F. Călțun, A. R. Iordan, M. N. Palamaru, *The influence of the chelating/combustion agents on the structure and magnetic properties of zinc ferrite*, *Cent. Eur. J. Chem* 10(6) (2012) 1799-1807.
- [28] A. Bjornerud, *The physics of magnetic resonance imaging*, University of Oslo, 2008.

### List of ISI publications:

1. **C. P. Constantin**, T. Slătineanu, M. Palamaru, A. Iordan, O. F. Călțun, *Co<sub>x</sub>Zn<sub>x-1</sub>Fe<sub>2</sub>O<sub>4</sub> nanoparticles ferrite series as magnetic resonance imaging contrast agents*, *Digest Journal of Nanomaterial and Biostructures*, 7(4) (2012) 1793-1798.
2. Tamara Slatineanu, Alexandra Raluca Iordan, Victor Oancea, Mircea Nicolae Palamaru, Ioan Dumitru, **Cristin Petrica Constantin**, Ovidiu Florin Caltun, *Magnetic and dielectric properties of Co-Zn*, *Materials Science and Engineering: B* 16(178) (2013) 1040-1047.
3. A. Doagă, A. M. Cojocariu, **C. P. Constantin**, R. Hempelmann, O. F. Călțun, *Magnetic nanoparticles for medical applications: progress and challenges*, AIP Proceed – acceptat spre publicare.

### **List of non-ISI publications:**

1. **C. P. Constantin**, A. Doaga, A. M. Cojocariu, I. Dumitru, O. F. Caltun, *Improved contrast agents for magnetic nuclear resonance medical imaging*, Journal of Advanced Research in Physics 2(2) (2011) 011106.

2. Anamaria Doagă, **Cristin P. Constantin**, Alina Cojocariu, Iordana Astefanoaei, Ioan Dumitru, Ovidiu F. Călțun, Phenomenological study of thermal field generated by nanoparticles arrays in hypertermia as treatment method, Journal of Advanced Research in Physics 2(1) (2011) 011110.

### **List of participations in international conferences**

- 20 presentations